Estimates of Thermal and Seismic Noise for Silicon Suspension Systems

Jahaira Valencia*

Department of Physics, Humboldt State University, Arcata, CA

(Dated: September 18, 2021)

Abstract

The project focused on finding estimates of thermal and seismic noise for silicon suspension systems at cryogenic temperatures. The motive of this study is due to the cryogenic upgrades planned for the $10m$ interferometer at the University of Glasgow. These calculations are the first step in the design of the $10m$ upgrades. A plot was successfully created using Python (Figure. 4) for the thermal displacement noise of a simplified mass on a spring/pendulum system. Unfortunately, the seismic noise estimates were not completed due to lack of time in a 10-week program. The steps on finding the seismic noise estimate are shown in the "future work" section. The Python code was then passed on to my mentor, Dr. Giles Hammond, to continue to project.

I. INTRODUCTION

This summer I worked with Dr. Giles Hammond from the University of Glasgow on a project dedicated to estimating the thermal and seismic noise of multi-stage suspension systems for gravitational wave detectors. The motivation for my project is due to the cryogenic upgrades planned for the $10m$ interferometer located at the University of Glasgow. Specifically, these upgrades stem from the fact that mirror thermal noise is a dominant noise source at room temperatures and reduction of it will improve the sensitivity of gravitational wave detectors.

For the first few weeks of the program, I read as much as I could about aLIGOs' fused silica quasi-monolithic suspension system shown in Fig. 1. Although Silica is not a good candidate for cryogenic temperatures, it was important to understand the upgrades from initial LIGO to begin to think about the design of the new suspension system for the $10m$ prototype.

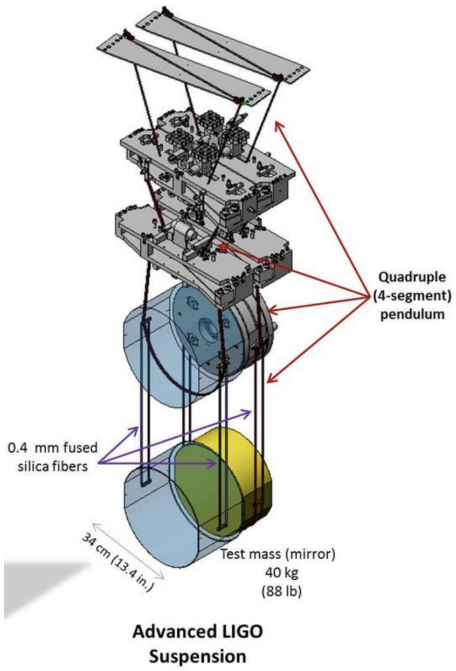

FIG. 1: The figure shows aLIGOS' fused Silica quasi-monolithic suspension system. The first 3 stages have springs that metal fibers are then suspended from. The test mass is then suspended from fused silica fibers due to the lower energy of the molecules within the material, reducing unwanted noise in the mirrors.

The suspension is composed of a 4-segment pendulum. The first 3 grey objects have springs that metal fibers are then attached to, while the test mass is suspended from (4) fused silica fibers. This is because the molecules in silica are less energetic than the molecules in the metal. Therefore, the thermal noise introduced to the test mass is reduced by suspending it with silica fibers. The mechanical dissipation of the system gives rise to thermal displacement noise. Therefore, mechanical loss is a key material property that defines thermal noise performance.

For seismic isolation, aLIGO has "passive" and "active" isolation systems. The passive systems arise due to the principles of pendulums, each link acts as a shock observer. The noise falls off as $1/f^2$ for each stage, hence 4 stages means the noise is reduced by a factor of $1/f^8$. For the active system, actuators apply a counteractive force to components of the suspension that compensate for unwanted physical vibrations.

I also spent a lot of time learning about the KAGRA suspension system, shown in Fig. 2, due to its' operations at cryogenic temperatures.

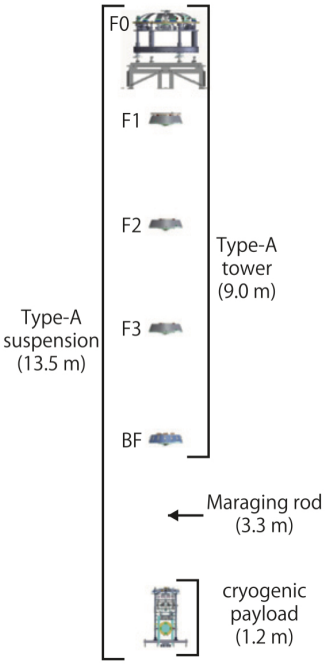

FIG. 2: KAGRA 9-stage suspensions system is composed of the Type-A tower, the first 5 stages, which operates at room temperature and a cryogenic payload, last 4 stages, that operates at $T = 20K$

The first five stages of KAGRA: $F_0, F_1, F_2, F_3,$ *and* BF, are called the "type-A tower" and operate at room temperature. The lower four stages are called the "cryogenic payload", which operates at $T = 20K$, shown in Fig. 3.

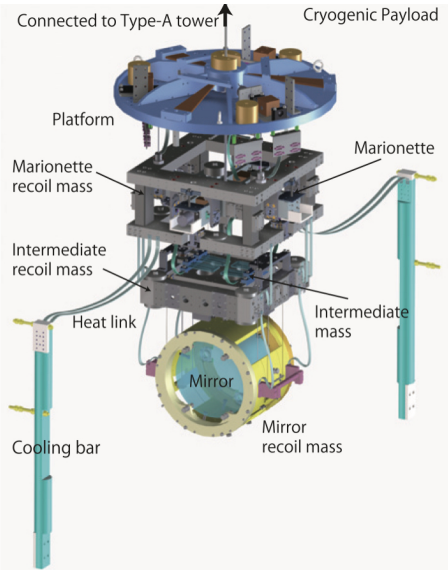

FIG. 3: The cryogenic payload is composed of a test mass chain surrounded by its' corresponding recoil masses (RM's). The test mass chain includes the Marionette mass (MN), Intermediate mass (IM), and the Test mass (TS).

The cryogenic payload has two chains, a test mass chain (TM) and a recoil mass chain (RM) that are independently suspended from the platform (PF). The test mass chain includes the marionette mass (MN), Intermediate mass (IM), and the Test mass (TM) which are all surrounded by their corresponding recoil mass. The cryogenic payload also has 3 different kinds of local sensors to control the suspensions: angular sensing optical levers (OPlevs), length sensings OPlevs, and photo-reflective displacement sensors. Similar to aLIGO, there are actuators on the cryogenic payload to counteract unwanted vibrators. KAGRA is also underground, which in itself provides seismic isolation. The 9-stage system indicates that the seismic noise on the test mass is reduced by a factor of $1/f^{18}$.

Although there is much more detail that I simply do not have space to include, learning about these suspension systems provided a good background to start thinking about the designs for the $10m$ upgrade. Starting with a simplified model of a mass on a spring, an expression for the thermal displacement noise for the pendulum, vertical, and violin modes were found (Equations 7, 20, and 24). As previously stated, the mechanical loss of the

system is a key property that defines the thermal noise, so the total mechanical loss was also found for the pendulum, vertical, and violin modes. The resonant frequencies for the 3 modes were also investigated. A python code was then created to map out the thermal displacement noise of the pendulum, vertical, and violin mode together.

An estimate for the seismic noise was also attempted, but due to timing restrictions was not completed. There is more detail about the seismic noise calculations in the "future work" section.

II. METHODS: PENDULUM MODE

A. Derivation of Thermal Displacement Loss for Pendulum Mode

First, an equation for the thermal displacement noise, $X(\omega)$, was derived using Eq. 1 to analyze the thermal noise of the suspensions in the pendulum mode. S_x is the power spectra density, K_B is Boltzmann constant, T is temperature, ω is the angular frequency, and $R[Y(\omega)]$ is the real part of the admittance. Eq. 2 shows the relationship between the admittance, $Y(\omega)$, and the impedance, $Z(\omega)$, while Eq. 3 shows the mechanical impedance used for the derivation where F is the net force and $\dot{x}$ is the velocity of a mass in a spring system.

$$S_x(\omega) = \frac{4k_B T}{\omega^2} R[Y(\omega)] \tag{1}$$

$$Y(\omega) = \frac{1}{Z(\omega)} \tag{2}$$

$$Z(\omega) = \frac{F}{\dot{x}(\omega)} \tag{3}$$

The analysis begins by thinking about the equation of motion for a mass, m, on a spring with drag coefficient b and spring constant k, shown in Eq. 4. This is a second order linear ordinary differential equation and governs the motion of this mass-spring oscillator.

$$F = m\ddot{x} + b\dot{x} + kx \tag{4}$$

The goal is to find the mechanical impedance of a spring-mass system by using the solution of Eq. 4 and some algebraic manipulation. Finding the mechanical impedance will

allow us to find the admittance, and in turn the power spectra density. First, we divide by m on both sides which results in Eq. 5. Let $\gamma = \frac{b}{m}$ and $\omega_o^2 = \frac{k}{m}$, where γ is the damping coefficient and ω_o is the resonant frequency of the pendulum mode.

$$\frac{F}{m} = \ddot{x} + \gamma\dot{x} + \omega_o^2 x \tag{5}$$

The solution to Eq.5 takes the form of $x = x_o e^{i\omega t}$, the first and second derivatives are shown below.

Solution to equation of motion for spring-mass system and it's derivatives:

$$\begin{aligned} x(\omega) &= x_o e^{i\omega t} \\ \dot{x}(\omega) &= i\omega x_0 e^{i\omega t} \\ &= i\omega x \\ \ddot{x}(\omega) &= (i\omega)^2 x_o e^{i\omega t} \\ &= i\omega\dot{x} \end{aligned}$$

Next, we insert $\ddot{x}$ and x back into Eq. 5 and multiply the left hand side by $\frac{i\omega}{i\omega}$ to allow the whole expression to be in terms of $\dot{x}$. This step will allow us to easily manipulate the expression to result in the form of the admittance, as shown below.

Find the admittance:

$$\frac{F}{m} = \ddot{x} + \gamma\dot{x} + \omega_o^2 x$$

$$= i\omega\dot{x} + \gamma\dot{x} + \omega_o^2(x_o e^{i\omega t}) \times \frac{i\omega}{i\omega}$$

$$= \frac{-\omega^2\dot{x} + i\omega\gamma\dot{x} + \omega_o^2 i\omega x_0 e^{i\omega t}}{i\omega} \quad (\text{ where } i\omega x_0 e^{i\omega t} = \dot{x})$$

$$= \frac{-\omega^2\dot{x} + i\omega\gamma\dot{x} + \omega_o^2\dot{x}}{i\omega}$$

$$\frac{F}{\dot{x}} = -\omega^2 + i\omega\gamma + \omega_o^2\left(\frac{m}{i\omega}\right) \quad (\text{Recall } Z(\omega) = \frac{F}{\dot{x}(\omega)} \text{and } Y(\omega) = \frac{1}{Z(\omega)})$$

$$\boxed{Y(\omega) = \frac{i\omega}{m}\frac{1}{((\omega_o^2 - \omega^2) + i\omega\gamma)}}$$

Next, we must identify a relationship between γ and the mechanical loss, θ, of the spring-mass system. By comparing the second line below to Eq. 5 we can easily see the relationship between γ and all the other parameters. This step will be crucial further into the derivation.

Force on a mass-spring system accounting for mechanical loss:

$$F_{spring} = -k(1 + i\theta)x$$

$$F_{net} = m\ddot{x} + k(1 + i\theta)x$$

$$= m\ddot{x} + ik\theta x + kx$$

Recall $F = m\ddot{x} + b\dot{x} + kx$

$\therefore\ ik\theta x = b\dot{x}\ and\ \dot{x} = i\omega x$

$ik\theta x = bi\omega x$

$k\theta = b\omega$

$b = \frac{k\theta}{\omega}\ \therefore \gamma = \frac{b}{m} = \frac{k\theta}{\omega m}$

$$\boxed{\gamma = \frac{k\theta}{\omega m}}$$

Finally, the steps to find the real part of the admittance and in turn find an expression for $S_x(\omega)$ are shown below. The power spectra density has units of $\frac{m^2}{Hz}$ which means we can obtain $X(\omega)$ by simply taking the square root of $S_x(\omega)$, as shown in Eq. 6.

$$X(\omega) = \sqrt{S_x(\omega)} \tag{6}$$

Find real part of admittance and thermal displacement noise:

$$Y(\omega) = \frac{i\omega}{m}\frac{1}{((\omega_o^2 - \omega^2) + i\omega\gamma)} \text{ (multiply by complex conjugate)}$$

$$= \frac{i\omega}{m}[\frac{1}{((\omega_o^2 - \omega^2) + i\omega\gamma)} \times \frac{((\omega_o^2 - \omega^2) - i\omega\gamma)}{((\omega_o^2 - \omega^2) - i\omega\gamma)}]$$

$$= \frac{i\omega}{m}[\frac{(\omega_o^2 - \omega^2) - i\omega\gamma}{(\omega_o^2 - \omega^2)^2 + \omega^2\gamma^2}]$$

$$= \frac{i\omega(\omega_o^2 - \omega^2) + \omega^2\gamma}{m[(\omega_o^2 - \omega^2)^2 + \omega^2\gamma^2]} \text{ (Now take the real part)}$$

$$R[Y(\omega)] = \frac{\omega^2\gamma}{m[(\omega_o^2 - \omega^2)^2 + \omega^2\gamma^2]} \text{ (Recall } \gamma = \frac{k\theta}{\omega m})$$

$$= \frac{\omega k\theta}{m^2[(\omega_o^2 - \omega^2)^2 + \omega^2(\frac{k\theta}{\omega m})^2]} \text{ (Recall } \omega_o^2 = \frac{k}{m})$$

$$= \frac{\omega\omega_o^2\theta}{m[(\omega_o^2 - \omega^2)^2 + \omega_o^4\theta^2]} \text{ (Recall } S_x(\omega) = \frac{4k_BT}{\omega^2}R[Y(\omega)])$$

$$S_x(\omega) = \frac{4k_BT}{\omega m} \times \frac{\omega_o^2\theta}{[(\omega_o^2 - \omega^2)^2 + \omega_o^4\theta^2]}$$

$S_x(\omega) = X(\omega)^2$ where $X(\omega)^2$ is the thermal noise displacement

$X(\omega) = \sqrt{S_x(\omega)}$

$\therefore$ **Thermal Displacement Noise is**

$$X(\omega) = \sqrt{\frac{4k_BT}{\omega m} \times \frac{\omega_o^2\theta_{pendulum}}{[(\omega_o^2 - \omega^2)^2 + \omega_o^4\theta_{pendulum}^2]}} \tag{7}$$

The thermal displacement noise is dependent on the resonant frequency, ω_o, the frequency of interest, ω, the mass of the object, m, the temperature operating at, T, and the mechanical loss of the pendulum, $\theta_{pendulum}$. First, an estimate for the resonant frequency can be found by thinking about a simple pendulum. The resonant frequency is then dependent on the length of the pendulum and the gravity of Earth, as shown in Eq. 8.

$$\omega_o = \sqrt{\frac{g}{L}} \tag{8}$$

$$\omega_o = 2\pi f_o \tag{9}$$

B. Mechanical Loss for Pendulum Mode

In order to find the mechanical loss of the pendulum, we must first find an estimate for the mechanical loss of the fiber, θ_{fiber}. The mechanical loss of the fiber is composed of two components: the loss that arises at the surface of the fiber and the thermoelastic loss as described in Eq. 10.

$$\theta_{fiber} = \theta_{surface} + \theta_{thermoelastic} \tag{10}$$

Eq. 11 is used to find the surface loss, where $h\theta_s$ is the surface loss constant (Table. I) and d is the diameter of the fiber (Table. IV).

$$\theta_{surface} \approx \frac{8h\theta_s}{d} \tag{11}$$

$$d = 2r \tag{12}$$

To obtain an expression for the radius we must think about the static stress, σ, applied on the fiber. The stress is the force divided by the area of the fiber, where the force is equal to mass times accelerations and the area is that of a circle as shown below. It is important to note that the mass is $\frac{m}{n}$ because there are n fibers attached to the test mass ($n = 4$).

Derivation of radius equation:

$$\sigma = \frac{F}{A}$$

$$= \frac{\frac{m}{n}g}{\pi r^2}$$

$$\boxed{r = \sqrt{\frac{m}{n}\frac{g}{\pi\sigma}}} \text{ where n=4 fibers} \tag{13}$$

The thermoelastic loss is due to the bending of the fiber that suspends the test mass, the expression for it is shown in Eq. 14. Y is Young's Modulus, T is the temperature, ρ is the density, C is the specific heat capacity, α is the coefficient of linear thermal expansion, σ is the static stress, ω is frequency of interest, and τ is the characteristic heat flow time (Eq. 15), where d is the diameter of the fiber and K is the thermal conductivity.

$$\theta_{th}(\omega) = \frac{YT}{\rho C}(\alpha + \sigma\frac{\beta}{Y})^2\frac{\omega\tau}{1+(\omega\tau)^2} \tag{14}$$

$$\tau = \frac{1}{4.32\pi}\frac{\rho C d^2}{K} \tag{15}$$

The total mechanical loss of the pendulum system is actually less than the mechanical loss of the fiber due to a significant amount of energy being stored in the lossless gravitational field. Therefore, to find the total loss of the system we must divide the loss of the fiber by the dilution factor, D, as shown in Eq. 16. Eq. 17 shows the expression for the dilution factor, where L is the total length of the pendulum, T is the tension on the fiber (Eq. 18), n is the number of fibers ($n = 4$), Y is Young's modulus, and I is the moment of cross sectional area (Eq. 19).

$$\theta_{pendulum} = \frac{\theta_{fiber}}{D} \tag{16}$$

$$D = \frac{2L\sqrt{T}}{n\sqrt{YI}} \tag{17}$$

$$T = \frac{mg}{n} \tag{18}$$

$$I = \frac{\pi r^4}{4} \tag{19}$$

Finally, all of the expressions necessary to design a code that will map the thermal displacement noise of the pendulum mode have been found. Some of the parameters discussed earlier are coded as variables to allow easy manipulation of the values for optimization, such as the value of the test mass and the total length of the pendulum. However, other values are dependent on the material used. For Cryogenic purposes, Silicon is a good candidate and some of the properties are shown in Table. I.

C. Parameter Values for Thermal Noise Plots

Material properties	**Silicon T=123K**
Surface Loss Constant, $h\theta_S$	$5 \times 10^{-13}\ m$
Density, ρ	2330 Kgm^{-3}
Young's Modulus, Y	$167 \times 10^9 Pa$
Coefficient of Thermal Expansion, α	$2.4 \times 10{-}8\ K^{-1}$
Thermal Conductivity, K	1.45 W/mK
Specific Heat Capacity, C	711 J/K
Thermoelastic Coefficient, β	$-1.9 \times 10^{-5} k^{-1}$
Surface loss constant, $h\theta_s$	$5 \times 10^{-13} m$

TABLE I: Silicon material properties that are hard coded in Python

Code Variables	Values
Stress,σ	$30MPa$
Total Length of Pendulum, $L = l_n \times n$	$L = 20Cm \;\; n = 2 \; or \; n = 3$
Mass, m	$1kg$
Frequency of interest, $f = \omega/(2\pi)$	$.1 - 100Hz$
Mass of the fiber, m	$1Kg$

TABLE II: Adjustable code variables in python

III. METHODS: VERTICAL AND VIOLIN MODES

A. Thermal Displacement Noise Vertical Mode

The suspension fibers can be thought about as stiff springs, like any other spring this will give rise to the "vertical" or "bounce" mode due to the restorative force. Eq. 20 shows the expression for the thermal displacement noise of the vertical mode, $X_v(\omega)$, where ω_v is the resonant frequency and $\theta_v(\omega)$ is the mechanical loss. The value .001 is the accepted conservative estimate of vertical to horizontal motion cross coupling due to the earths' curvature. K_B, T, m, and ω are the same parameters as the thermal displacement noise for the pendulum mode.

$$X_v(\omega) = .001\sqrt{\frac{4K_BT}{m\omega}\left(\frac{\omega_v^2\theta_v(\omega)}{\omega_v^4\theta_v^2(\omega) + (\omega_v^2 - \omega^2)^2}\right)} \tag{20}$$

Similar to the pendulum mode, estimates for the resonant frequency are necessary to obtain the thermal displacement noise. To find an expression for ω_v, we must think about the force exerted by stretched or contracted material as shown on the third line below. An expression to solve for the spring constant can be found by comparing the stretch force to Hooke's law. The spring constant will then allow us to estimate the resonant frequency as shown in Eq. 22.

Derivation for resonant frequency of vertical mode:

$$Y = \frac{\sigma}{\epsilon}$$

$$= \frac{F}{A}\frac{L}{\Delta L}$$

$$F = YA\frac{\Delta L}{L}$$

$F = k\Delta L$ Hooke's law

$\therefore$ by comparison

$$\boxed{k = \frac{YA}{L}} \tag{21}$$

$$F = m\ddot{x} + b\dot{x} + kx$$

$\therefore$

$$\omega_v^2 = \frac{k}{m}$$

$$m = m/4$$

$$\boxed{\omega_v = \sqrt{\frac{4k}{m}} \text{ and } f_v = \sqrt{\frac{4k}{m}}/2\pi} \tag{22}$$

Next, an estimate of the mechanical loss of the vertical mode is required according to Eq. 20. In this case, the thermoelastic loss can be neglected due to the fact that the fibers do not bend in the vertical mode. The total mechanical loss is merely the surface loss, Eq. 23. All the expressions to plot the thermal displacement noise of the vertical mode have been derived and solved for, the plots will be shown in the "Results" section.

$$\theta_v(\omega) \approx \theta_{surface}(\omega) \approx \frac{8h\theta_s}{d} \tag{23}$$

B. Thermal Displacement Noise for Violin Mode

The violin modes, excitation of transverse modes of vibrations of the suspended fibers, can lead to motion of the test mass. This motion can then be sensed by the interferometer and documented at its' output signal for many harmonics. Eq. 24 shows the expression needed to find the thermal displacement noise for the j^{th} violin mode where m_{fiber} is the mass of the fiber, $\omega_{vio\,j}$ is the resonant angular frequency for the j^{th} mode, and θ_{vio} is the mechanical loss. The other terms in the expression are the same as the previous thermal displacement noise equations (Eq. 7 and Eq. 20).

$$X_{violin\,j}(\omega) = \sqrt{\frac{4K_BT}{\omega}\frac{2m_{fiber}}{\pi^2 m^2 j^2}\left(\frac{\omega_{vio\,j}^2\theta_{vio}}{\omega_{vio\,j}^4\theta_{vio}^2 + (\omega_{vio\,j}^2 - \omega^2)^2}\right)} \; for\ the\ j^{th}\ individual\ violin\ mode \tag{24}$$

Similarly to the pendulum and vertical modes, estimates for the resonant frequency, Eq. 25, are required for the first 3 violin modes. A small derivation of the resonant frequency for $j = 1$ is shown below where T (Eq. 18) is the tension of each string, μ is the linear density of the fiber (Eq. 30), and L is the total length of the pendulum. Eq's. 26 and 27 show the expressions used to find the resonant frequency for the second and third violin mode.

Resonant frequency for j is 1:

$$c = f\lambda$$

$$\lambda = 2L$$

$$\therefore$$

$$f = \frac{c}{2L}$$

$$\therefore$$

$$f_{vio1} = \frac{\sqrt{\frac{T}{\mu}}}{2L} \tag{25}$$

$$f_{vio2} = 2 \times f_{vio1} \tag{26}$$

$$f_{vio3} = 3 \times f_{vio1} \tag{27}$$

$$\omega_{vio\ j} = 2\pi f_{vio\ j} \tag{28}$$

The mechanical loss of the violin mode is twice that of the pendulum mode as shown in Eq. 29. Eq. 31 shows the expression to find the mass of the fiber where r is the radius, L is the length of the pendulum, and ρ is the density of silicon.

$$\theta_{vio} = 2 \times \theta_{pendulum} \tag{29}$$

$$\mu = \pi r^2 \rho \tag{30}$$

$$m_{fiber} = \pi r^2 L \rho \tag{31}$$

Finally, the thermoelastic noise for the pendulum, vertical, and violin modes $j = 1, 2, 3$ were plotted and shown in Fig. 4.

IV. RESULTS

Resonant Frequency	**Variable**	**Value**
Pendulum mode	f_o	$1.11Hz$
Bounce mode	f_v	$83.16Hz$
First violin mode	f_{vio1}	$283.67Hz$
Second violin mode	f_{vio2}	$567.35Hz$
Third violin mode	f_{vio3}	$851.02Hz$

TABLE III: Resonant frequency values for all modes

Name	**Variable**	**Value**
Tension	T	$2.4525\ N$
Diameter of fiber	d	$0.000322\ m$
Dilution factor	D	16.617
Surface loss	$\theta_{surface}$	1.239×10^{-8}

TABLE IV: Values obtained using the specific silicon material properties and values from table. II

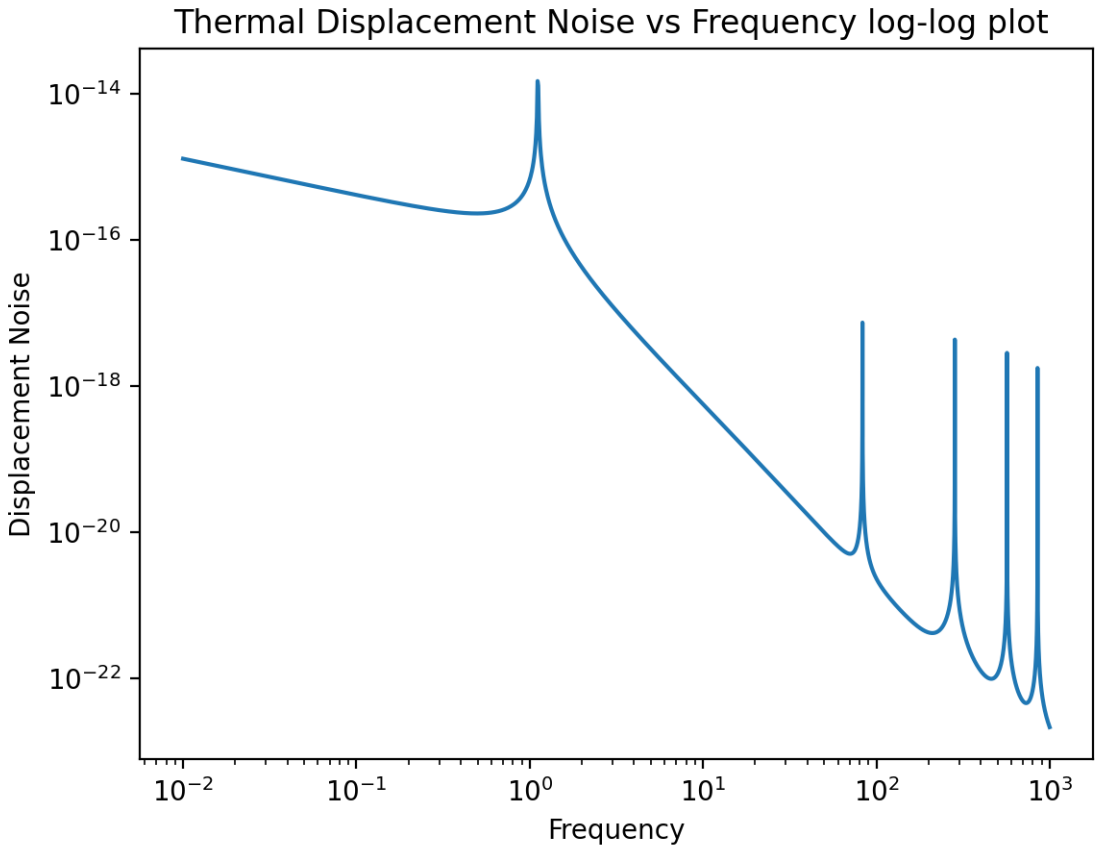

FIG. 4: Thermal displacement noise plot of pendulum (first peak), vertical (second peak), and violin modes (3rd,4th, and 5th peak) all together.

V. ANALYSIS

Table III shows the results for the resonant frequencies of each mode of interest, found by using values from Tables II and IV. Table IV shows values obtained via the coding process for tension of the fibers, diameter of the fibers, surface loss, and the dilution factor. The resonant frequency values are kind-of arbitrary on their own until optimization of suspension parameters are found. However, they help provide a plot to start understanding what the thermal noise looks like for these suspension systems at cryogenic temperatures.

Fig. 4 shows the pendulum mode (first peak), vertical mode (second peak), and first 3 harmonics of the violin mode together (3rd, 4th, and 5th peaks) in log space. Each peak corresponds to the resonant frequency of the respective mode. The plot shows that the vertical and violin modes do not change the slope of the pendulum mode, they simply add

some "annoying" spikes to the noise. This means that the pendulum mode is the dominant source of thermal noise. Another observation is that the violin modes get closer together in log space because they are simply multiples of the first harmonic as described in Eq. 26 and 27. These results are the first step in being able to optimize some of the parameters such as: the length of the pendulum, the test mass value,the stress the fibers can support before breaking, and even the number of stages of the suspension system. The next steps and future work will be discussed in the next section.

VI. FUTURE WORK

The next step of this project would be to find an estimate for the seismic noise, which I did not have enough time to complete. The number of stages, n, for the upgrades to the $10m$ prototype suspension system at the University of Glasgow will probably only be 3 or 2 stages.

A. Seismic noise: Horizontal Isolation

First, we begin by thinking about the motion being restricted in a single axis, x, shown in Fig. 5. This will be the horizontal contributions of the seismic noise on the suspension system.

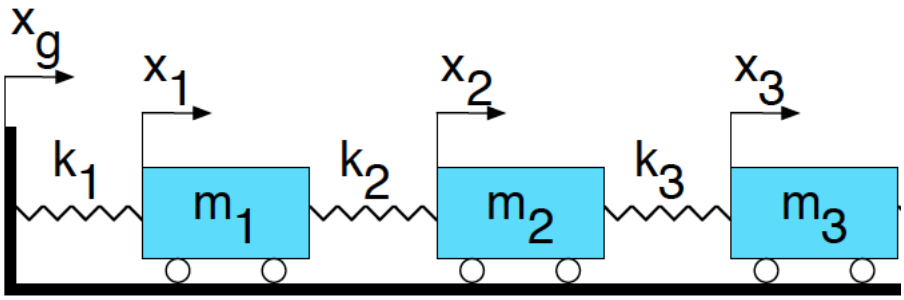

FIG. 5: Generalized multistage pendulum system used to think about the seismic noise isolation. The masses are constraint to moving in one single direction, x. x_g is the ground motion (also limited in movement in only the $x - axis$), x_1 to x_3 are the motions of the stages $1-3$, m_1 to m_3 are the mass of the stages, and finally k_1 to k_3 are the spring constants of the stages.

Equations 32 and 33 are required to find the transmission of seismic noise where x_3 and x_2 are the motion of stages n=3 and n=2 respectively, x_g is the ground motion, k_n is the spring constant for the respective stage, m_n is the mass of the stage, and f is the range of frequencies of interest $(.1 - 100Hz)$.

$$\text{for n=3} \ : \quad \frac{x_3}{x_g} = \frac{1}{(2\pi f)^6} \frac{k_1 k_2 k3}{m_1 m_2 m_3} \tag{32}$$

$$\text{for n=2} \ : \quad \frac{x_2}{x_g} = \frac{1}{(2\pi f)^4} \frac{k_1 k_2}{m_1 m_2} \tag{33}$$

An estimate for the springs constants can be found by using Eq. 34 where $l_i = l_n$ is the individual length of the stages. The relationship between the individual stage length, l_n, and the total length of the pendulum system , L, is shown in Eq. 35. It is important to note that the seismic noise falls of as $1/f^2$ for each stage. Hence 3 stages means the noise falls off as $1/f^6$ while 2 stages means the noise falls off as $1/f^4$.

$$k_n = g \sum_{i=1}^{n} \frac{m_i}{l_i} \tag{34}$$

$$l_n = \frac{L}{n} \tag{35}$$

B. Seismic Noise: Vertical Isolation

The expressions to find the transmission of seismic noise through the system in the vertical direction are shown in equations 36 and 37 where g is the gravity of earth, and l_1-l_3 are the length of the stages 1-3. These expressions can be used to find the optimization of the length of the stages and the mass of the stages.

$$\text{for n=3} \ : \quad \frac{x_3}{x_g} = \frac{g^3}{(2\pi f)^6} \frac{1}{l_1 l_2 l_3} \frac{(m_1 + m_2 + m_3)(m_2 + m_3)(m_3)}{l_1 l_2 l_3} \tag{36}$$

$$\text{for n=2} \ : \quad \frac{x_2}{x_g} = \frac{g^2}{(2\pi f)^4} \frac{1}{l_1 l2} \frac{(m_1 + m_2)(m_2)}{l_1 l_2} \tag{37}$$

The values for l_n were found by setting an arbitrary pendulum length $L = 20Cm$ (Table II) and dividing by the number of stages, n (Eq. 35). Each stage will be of equal length

and will make up the total length of the multistage pendulum. Estimates for the spring constant can be found by using Eq. 34.

C. Ground Motion

Unfortunately, I did not understand how to obtain an expression for the ground motion at the site of the $10m$ prototype at the University of Glasgow. For this very reason, I was unable to create a code that would map out the vertical and seismic noise for the multistage pendulum. I did create a code that would ideally plot the seismic noise with the assumption that x_g was in the form of $1/f^2$. Sadly, this is not a good approximation and the plots do not hold any valuable information so I will not include them in this paper. On a side note, the ground motion would also allow us to figure out at what resonant frequency our system needs to operate at. If we think about a single mass on spring, then the idea is that we can operate the system such that the ground motion is higher than the resonant frequency. In this case, the ground can bounce up and down very quickly but the mass and springs have inertia that inhibits the motion of the ground on the system. This is the case that gives seismic isolation in the form of $1/f^2$ and the concept can be used for multistage pendulum systems.

D. Other Future Work

Ideally, the seismic noise and the thermal noise plots would give us an opportunity to investigate how certain parameters, such as the length of the pendulum and the lengths of the individual stages, could affect either seismic or thermal noise. For example, the seismic noise falls off as $1/f^2$ for each stage. Naturally, one would think that large amount of short stages , like KAGRA, would mean better seismic isolation. However, according to my mentor Dr. Hammond, the thermal noise performance is better with longer stages.

As previously mentioned, in the suspension systems of aLIGO, some stages have springs and others do not. Our model and design will be similar, where some of the first stages will contain springs while the bottom stages will not. The next step would be to estimate the spring constants required for some known optimal value of spring resonant frequency that supports some known optimal value of mass using $\omega_o^2 = k/m$. Once an estimate for the

spring constant is known, then we can start thinking about how to design such a spring that operates in a vacuum system.

VII. ACKNOWLEDGEMENT

I would like to give a special thank you to Dr. Paul Faulda and Dr. Peter Wass for their continuous support throughout the 10-week program, as well as Dr. Guido Mueller for arranging the Europe and Florida travel plans. I would also like to thank Dr. Giles Hammond, my mentor, for creating a learning space that allowed me to ask questions whenever needed and supported me throughout the duration of the program. In addition, I would also like to thank the NSF grant numbers that funded the program: NSF PHY-1950830 and NSF PHY-1460803. This was truly an unforgettable experience that expanded my intellectual knowledge and provided me with a cultural experience I would have otherwise not come across.

VIII. REFERENCES

* jjv169@humboldt.edu

[1] Ushiba, Takafumi, et al. "Cryogenic suspension design for a kilometer-scale gravitational-wave detector." Classical and Quantum Gravity 38.8 (2021): 085013.

[2] Shapiro, Brett, Dakota Madden-Fong, and Brian Lantz. LIGO III Quad Pendulum Conceptual Design Optimization. Technical report, LIGO and Virgo Scientific Collaborations, https://dcc. ligo. org/LIGO-T1300786/public, 2014.

[3] Cumming, A. V., et al. "Silicon mirror suspensions for gravitational wave detectors." Classical and Quantum Gravity 31.2 (2013): 025017.

[4] Cumming, A. V., et al. "Lowest observed surface and weld losses in fused silica fibres for gravitational wave detectors." Classical and Quantum Gravity 37.19 (2020): 195019.

[5] Cumming, A. V., et al. "Design and development of the advanced LIGO monolithic fused silica suspension." Classical and Quantum Gravity 29.3 (2012): 035003.

[6] Cumming, A., et al. "Finite element modelling of the mechanical loss of silica suspension fibres for advanced gravitational wave detectors." Classical and Quantum Gravity 26.21 (2009): 215012.